Graphene Oxide Nanosheet with High Proton Conductivity

ARTICLE *in* JOURNAL OF THE AMERICAN CHEMICAL SOCIETY · MAY 2013

Impact Factor: 12.11 · DOI: 10.1021/ja401060q · Source: PubMed

JACS
JOURNAL OF THE AMERICAN CHEMICAL SOCIETY

Communication

pubs.acs.org/JACS

Graphene Oxide Nanosheet with High Proton Conductivity

Mohammad Razaul Karim,[†,‡] Kazuto Hatakeyama,[†] Takeshi Matsui,[†] Hiroshi Takehira,[†] Takaaki Taniguchi,[†,§] Michio Koinuma,[†,§] Yasumichi Matsumoto,[†,§] Tomoyuki Akutagawa,[∥] Takayoshi Nakamura,[⊥] Shin-ichiro Noro,[⊥] Teppei Yamada,[#] Hiroshi Kitagawa,[§,#] and Shinya Hayami*[,†,§]

[†]Graduate School of Science and Technology, Kumamoto University, 2-39-1 Kurokami, Kumamoto 860-8555, Japan

[‡]Department of Chemistry, School of Physical Sciences, Shahjalal University of Science and Technology, Sylhet-3114, Bangladesh

[§]CREST, Japan Science and Technology Agency (JST), 7 Gobancho, Chiyoda-ku, Tokyo 102-0076, Japan

[∥]Institute of Multidisciplinary Research for Advanced Materials (IMRAM), Tohoku University, 2-1-1 Katahira, Aoba-ku, Sendai 980-8577, Japan

[⊥]Research Institute for Electronic Science, Hokkaido University, N20W10 Kita-ku, Sapporo 001-0020, Japan

[#]Division of Chemistry, Graduate School of Science, Kyoto University, Kitashirakawa-Oiwakecho, Sakyo-ku, Kyoto 606-8502, Japan

Supporting Information

ABSTRACT: We measured the proton conductivity of bulk graphite oxide (GO′), a graphene oxide/proton hybrid (GO-H), and a graphene oxide (GO) nanosheet for the first time. GO is a well-known electronic insulator, but for proton conduction we observed the reverse trend, as it exhibited superionic conductivity. The hydrophilic sites present in GO as −O−, −OH, and −COOH functional groups attract the protons, which propagate through hydrogen-bonding networks along the adsorbed water film. The proton conductivities of GO′ and GO-H at 100% humidity were $\sim 10^{-4}$ and $\sim 10^{-5}$ S cm^{-1}, respectively, whereas that for GO was amazingly high, nearly 10^{-2} S cm^{-1}. This finding indicates the possibility of GO-based perfect two-dimensional proton-conductive materials for applications in fuel cells, sensors, and so on.

Chemical networks for rapid propagation of protons are constantly being researched worldwide since Rogers and Ubbelohde reported the phenomenon in 1950.[1] A wide range of applications in biological systems, fuel cells, sensors, and chemical filters are the pertinent reason behind the worldwide research on designing inert and faster proton conductors.[2] As a result, proton conductors based on organic and coordination polymers, such as hydrocarbon ionomers, acid-doped polymers, inorganic/organic nanohybrids, superprotonic solid acids, and acid/base ionic liquids, have been developed to date, and the typical conductivity ranges reported for Nafion, phosphates, carboxylic acids, and imidazoles are 10^{-1}−10^{-5}, 10^{-1}−10^{-4}, 10^{-5}−10^{-6} and 10^{-6}−10^{-8} S cm^{-1}, respectively.[3] Some ceramic materials with outstandingly high conductivities have been reported as well.[4] However, for fuel cell applications, besides high conductivity, it is vital that the material possesses constant activity under humid, hot, and acidic conditions.[5] Thus, an inert polymeric matrix is usually preferred as the foundation for designing an ionic conductor. In this report, we consider the possibility of graphene oxide (GO) as a potential vehicle to transport protons, as its stability is very high and it contains closely located oxygenated functional groups (−O−, −OH, and −COOH) that extend outward from the flat two-dimensional carbon network and seem to assemble into one-dimensional hydrogen-bonded channels for proton transport.[6] Previously, Jung et al.[7a] used bulk graphite oxide (GO′) as a filler for different polymer electrolytes, while Zarrin et al.[7b] observed higher conductivity in a sulfonic acid-functionalized GO′/Nafion composite than in powdered GO′. Later, Ravikumar and Scott developed sulfonated GO′ paper with appreciable conductivity.[8] However, all of these studies involved bulk samples, and the in-plane ionic conductivity of pure GO nanosheets is still unknown. In this work, we for the first time successfully measured the ionic conductivity along the surface of GO. Recently, graphene-based materials have promised diversified applications because of their outstanding adaptability and stable functional properties.[9] GO, the oxidized form of graphene, has randomly allocated nonconductive sp^3 carbon sites that are responsible for abolishing the electrical conductivity of graphene.[10] Therefore, in contrast to graphene, GO is an electronic insulator.[11] However, we found the reverse trend for proton conductivity: the measured conductivities of GO′ and a GO/proton hybrid (GO-H) are $\sim 10^{-4}$ and $\sim 10^{-5}$ S cm^{-1} respectively, whereas, that of GO is $\sim 10^{-2}$ S cm^{-1}.

GO′ is the bulk product, which was obtained by oxidizing graphite using a slight modification of Hummer's method [see the Supporting Information (SI)].[12] A water dispersion of single/multilayer discrete GO nanosheets was obtained by exfoliation of GO′ through ultrasonication, and the nanosheets were identified by atomic force microscopy (AFM) image and X-ray photoelectron spectroscopy (XPS) (Figure S1 in the SI). The GO-H hybrid was directly precipitated from the GO dispersion using hydrochloric acid.

The proton conductivity was measured by a quasi-four-probe method using an impedance/gain phase analyzer (Solaratron 1260/1296) over the frequency range from 1 to 4 MHz. The GO′ and GO-H powdered samples were compressed into pellets with a diameter of 2.5 mm and thicknesses of 0.64 and 0.66 mm, respectively; both sides of each pellet were attached

Received: January 30, 2013
Published: May 16, 2013

   dx.doi.org/10.1021/ja401060q | J. Am. Chem. Soc. 2013, 135, 8097−8100

to gold wire (50 μm diameter, Tanaka Kikinzoku Kogyo) with gold paste. Impedance measurements were executed under controlled temperature and humidity using an incubator (SH-221, ESPEC). For GO fabrication, a comb-shaped gold electrode was soaked with one drop of dilute GO dispersion and then vacuum-dried for 24 h. This resulted in a coating with a random distribution of single- and multilayer GO nanosheets. The measured resistance of the bare comb electrode was very high (>10^8 Ω), which confirmed the absence of any parasitic impedance contribution. Water uptake was confirmed by pressure-dependent uptake tracing (Figure S2) and thermogravimetric and differential thermal analysis (TG/DTA) (Figure S3).

Figure 1a,b shows Nyquist plots of the impedance for GO′ and GO-H, respectively. The traces formed by the real (Z') and

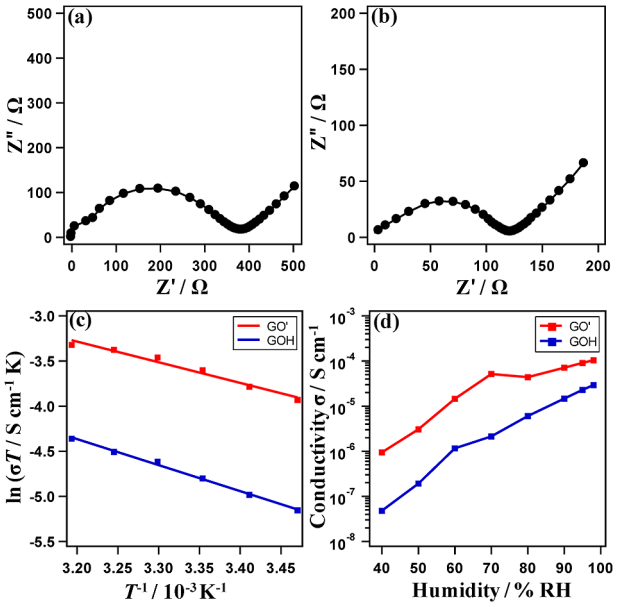

Figure 1. Nyquist plots of (a) GO′ and (b) GO-H at 100% RH and 300 K. (c) Plots of ln (σT) vs T^{-1} for GO′ and GO-H at 100% RH. (d) Proton conductivities (σ) of GO′ and GO-H with respect to RH at 300K.

imaginary parts (Z'') of the impedance as the frequency was varied were fit with distorted semicircular curves. The electric field dependence of the curves was evaluated, and the results at 100 mV turned out to be good. The diameters of the semicircles represent the resistances at the corresponding temperature and relative humidity (RH). The existence of the second circle indicates that the conductivity was driven by protons. The conductivity (σ) values were found to increase with temperature, and the linear fits of the plots of ln(σT) versus T^{-1} (Figure 1c) revealed activation energies (E_a) of 0.197 and 0.249 eV for proton conduction by GO′ and GO-H, respectively. The calculated σ values for GO′ and GO-H at 300 K and 100% RH were 1.3 × 10^{-4} and 2.9 × 10^{-5} S cm^{-1}, respectively, and decreased drastically with decreasing RH (Figure 1d). The σ value for GO′ matches with some previous reports.[13]

The temperature-dependent σ values confirmed that GO-H has a lower ionic conductivity than GO′ (Figure S4). Next, we measured the proton conductivity of GO on a comb-shaped electrode (Figure S5). The scanning electron microscopy (SEM) image (Figure 2a) shows the dispersion of GO on the

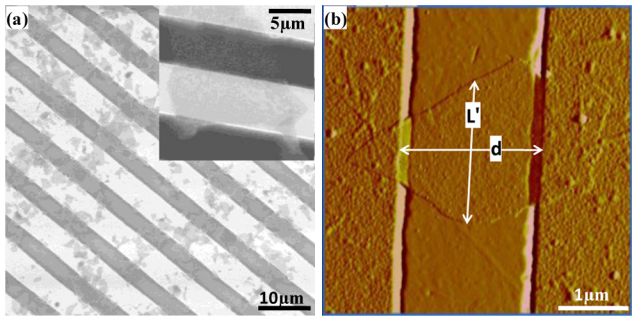

Figure 2. GO on comb electrode: (a) SEM image; (b) AFM image of a nanosheet bridging two opposite electrodes with an electrode separation d and a length component L'.

electrode surface and implies the existence of both single- and multilayer nanosheets. Statistical analysis revealed that almost 34% of the electrode surface was covered by GO. The effective length of the conductive film assembled from GO fragments was calculated from the summation of length components L' (Figure 2b) of nanosheets bridging the opposite electrodes only (see the SI). The dominance of the ionic conductivity was confirmed by the isotope effect at low temperature (<300 °C). The conductivity of H_2O-humidified GO was ∼1.25 times higher than that of D_2O-humidified GO (Figure 3a). Though

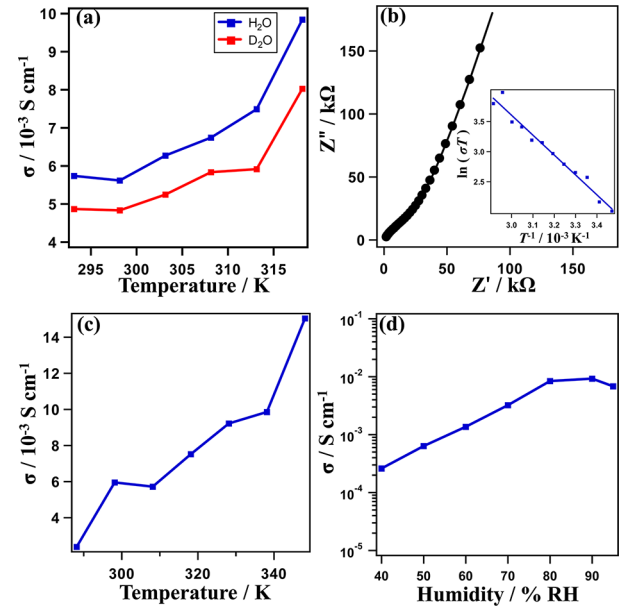

Figure 3. (a) Temperature-dependent conductivities of GO humidified by H_2O (blue) and D_2O (red) at 95% RH. (b) Nyquist plot of the impedance of GO and (inset) plot of ln(σT) vs T^{-1}. (c) Temperature-dependent conductivity at 95% RH at 100 mV. (d) Conductivity as a function of RH at 300 K.

this value is low, it agrees with the results of some previous works, where this ratio was reported to be 1.1−1.4 and 2−3.5 as evidence for proton-oriented conduction at low (<300 °C) and high temperature (>300 °C), respectively.[14] Also, the σ values for H_2O-humidified GO′ and GO-H pellets were ∼1.2 and ∼1.3 times higher than those for the corresponding D_2O-humidified samples (Figure S6). Figure 3b shows the Nyquist plot of the impedance data for GO. The E_a value obtained from the corresponding Arrhenius plot was 0.284 eV (Figure 3b inset).

dx.doi.org/10.1021/ja401060q | J. Am. Chem. Soc. 2013, 135, 8097−8100

Figure 3c presents the temperature dependence of the conductivity for the GO nanosheet assembly. The conductivity increased from 3.0×10^{-3} S cm^{-1} at 293 K to 1.5×10^{-2} S cm^{-1} at 360 K. This observation indicates σ for the sheet sample is stable at elevated temperature. Figure 3d shows that σ decreased from 7.0×10^{-3} S cm^{-1} at 95% RH to 4×10^{-4} S cm^{-1} at 40% RH.

Numerous reports suggest that proton conduction along nanoscale films is usually higher than in bulk compounds.[15] Mayer considered space charge, charge nonstoichiometries, and defect chemistry to explain the improved ionic conductivity of extremely thin films having thicknesses less than 4 times the Debye length.[16] GO with nanometer-range thickness can be characterized by similar criteria. In addition, we suggest that the conduction pathway for GO is similar to that for GO′ but is improved without any interference or restraint as in GO′. As a result, the proton conductivity for GO is amazingly high.

GO′ is basically a nonstoichiometric compound with a varying C:O:H ratio.[17] The extended oxygenated functional groups generate an interlayer spacing in GO′ that varies from ∼7.5 to ∼12 Å depending on the accommodation of the interlayer water film during humidification.[18] Negatively charged GO exerts repulsive forces, in contrast to the interlayer attraction in graphitic stacks. Therefore, the layer spacing in GO ensures more flexibility to promote the motion of water molecules and charge propagation. Buchsteiner and co-workers[18] reported that the hydration behavior of graphite materials is regulated mainly by the synthetic method (to control the number and distribution of oxygenated sites), the hydration process (to control the adsorption and distribution of water molecules), and the surface charge of the membrane layers. In the case of GO, the water molecules in the interlayer film remain stagnant through hydrogen bonding to the oxygenated functional groups of GO and undergo only localized motions, resulting faster proton movement. The high conductivity is also supposed to originate from the existence of both upstream and downstream fluxes of protons along the adsorbed water film with the functional groups on both the faces of GO foundation. The flux of protons along the hydrogen-bonding network is inversely proportional to the thickness of the membrane, and therefore, GO with nanometer-ranged thickness has a high σ value.

In addition, the absence of interlayer attractions in GO might be considered as a relevant issue for the high σ value. In the graphitic state, the parallel sheets are interconnected, whereas in the nanosheet assembly, layers are separated by ultrasonic exfoliation. The tiny exfoliated nanosheets are discrete, and hence, we propose that the hydrogen-bonding network of adsorbed water molecules and oxygenated sites on the GO nanosheet is free from any type of interruption originating from interlayer interactions. As a result, in GO there is no chance for the force driving both the forward movement of protons and the backward movement of oxygen vacancies to be perturbed. All of these facts are unique in GO and facilitate the faster ionic movement. The turbostratic stacking of layers restricts the proton conduction pathway in GO′.[19]

The σ values for GO-H are lower because some hydrophilic sites are blocked. During acid treatment, some of the negatively charged oxygenated sites in GO are neutralized by bonding with H^+, which results in discontinuities within the conductive channels. Hence, the frequency of hydrogen-bond breaking and reformation is altered. This barrier is more significant than that inflicted by turbostratic stacking of GO′, causing GO-H to have the lowest conductivity.

For GO, the σ value represents the in-plane conductivity. In GO′, however, the particles are randomly ordered, and σ should be a combination of the in-plane and through-plane conductivities. Moreover, GO′ contains numerous small interparticle gaps that are affected by some operative facts like the pressure applied to make the pellet. Therefore, we propose that the conductivity of the bulk sample has lower analytical accuracy and precision. However, this fact is reflected by the difference between the σ value reported here for our bulk sample and that reported by Zarrin et al.[7b] In this context, the achievement of a conductivity in the nanosheet assembly that is several orders of magnitude higher than that for same sample in the bulk indicates the possibility to obtain more accurate and increased σ values in other graphene-based materials following the measurement technique reported here. We also found significant evidence to avail improved conductivity in the future.

First, in some spots on the comb electrode, we detected multilayer deposition, the extent of which varied anomalously in repeated experiments, and the conductivity was found to increase with the ratio of the areas occupied by multilayer versus single-layer nanosheets. This indicates that higher conductivity can be obtained from multilayer fabrication. Previously, Matsui et al.[20] observed a similar trend in a multilayer polymer electrolyte. Second, the irregular shape of the tiny GO islands contributes to some slower movement of protons. We are currently trying to overcome this limitation through Langmuir−Blodgett (LB) assembly on the comb electrode. Previously, an LB film of a GO monolayer on a hydrophilic substrate was reported by Cote et al.[21] Finally, in our recent report, we proposed a model for epoxy-group-supported proton conduction in GO.[22] Therefore, we believe that increasing the number of epoxy sites might be a feasible way to increase the ionic conductivity of GO.

In conclusion, our current findings demonstrate the development of proton conductors based on a flat carbon skeleton. GO, GO′, and GO-H were synthesized through facile, quick, and reproducible methods. The measured conductivity displayed the trend GO > GO′ > GO-H. The conductivity of GO is 2−3 orders of magnitude greater than GO′. The fact that the E_a value complies with Grotthuss mechanism indicates practical applications of GO in the future. Besides, the present evidence indicates the possibility of better results for multilayer LB films of epoxy-rich GO. The conduction mechanisms in nanosheets and powdered samples are significantly different. For the nanosheet assembly, the σ value originates from in-plane protonic movement, whereas for the bulk sample, there should be a significant contribution from the through-plane conductivity. The solid-phase structure of GO confirms a privilege over other conductors such as phosphoric acid. Pure GO is obviously cheaper and more environmentally friendly than its hybrids or derivatives. In the near future we are waiting for the development of multilayer GO sheets as a solid electrolyte.

■ ASSOCIATED CONTENT

Ⓢ Supporting Information

Synthetic procedures, XPS spectrum of GO, water uptake measurements, TG/DTA data, calculation methods, SEM images, and temperature-dependent conductivities. This ma-

dx.doi.org/10.1021/ja401060q | J. Am. Chem. Soc. 2013, 135, 8097−8100

terial is available free of charge via the Internet at http://pubs.acs.org.

AUTHOR INFORMATION

Corresponding Author

hayami@sci.kumamoto-u.ac.jp

Notes

The authors declare no competing financial interest.

ACKNOWLEDGMENTS

This work was supported by Innovative Areas "Coordination Programming" (Area 2107) from MEXT, Japan.

REFERENCES

(1) Rogers, S. E.; Ubbelohde, A. R. *Trans. Faraday Soc.* **1950**, *46*, 1051−1061.

(2) (a) Voth, G. A. *Acc. Chem. Res.* **2006**, *39*, 143−150. (b) Royant, A.; Edman, K.; Ursby, T.; Pebay-Peyroula, E.; Landau, E. M.; Neutze, R. *Nature* **2000**, *406*, 645−648. (c) Kreuer, K. D. *Chem. Mater.* **1996**, *8*, 610−641. (d) Kudo, T.; Fueki, K. *Solid State Ionics*, 1st ed.; VCH: Weinheim, Germany, 1990.

(3) (a) Bose, S.; Kuila, T.; Nguyen, T. X. H.; Kim, N. H.; Lau, K.-t.; Lee, J. H. *Prog. Polym. Sci.* **2011**, *36*, 813−843. (b) Yang, L.; Tang, J.; Li, L.; Chen, X.; Ai, F.; Yuan, W. Z.; Wang, L.; Zhang, Y. *RSC Adv.* **2012**, *2*, 5950−5953. (c) Vilčiauskas, L.; Tuckerman, M. E.; Bester, G.; Paddison, S. J.; Kreuer, K. D. *Nat. Chem.* **2012**, *4*, 461−466. (d) Woundenberg, R. C.; Yavuzcetin, O.; Tuominen, M. T.; Coughlin, E. B. *Solid State Ionics* **2007**, *178*, 1135−1141. (e) McKeen, J. C.; Yan, Y. S.; Davis, M. E. *Chem. Mater.* **2008**, *20*, 5122−5124. (f) Kreuel, K. D. *J. Membr. Sci.* **2001**, *185*, 29−39.

(4) Pergolesi, D.; Fabbri, E.; Epifanio, A. D.; Bartolomeo, E. D.; Tebano, A.; Sanna, S.; Licoccia, S.; Balestrino, G.; Traversa, E. *Nat. Mater.* **2010**, *9*, 846−852.

(5) Zhang, H.; Shen, P. K. *Chem. Rev.* **2012**, *112*, 2780−2832.

(6) (a) Jeong, H. K.; Noh, H. J.; Kim, J. Y.; Jin, M. H.; Park, C. Y.; Lee, Y. H. *EPL* **2008**, *82*, No. 67004. (b) Mkhoyan, K. A.; Contryman, A. W.; Silcox, J.; Stewart, D. A.; Eda, G.; Mattevi, C.; Miller, S.; Chhowalla, M. *Nano Lett.* **2009**, *9*, 1058−1063. (c) Szabo, T.; Berkesi, O.; Forgo, P.; Josepovits, K.; Sanakis, Y.; Petridis, D.; Dekany, I. *Chem. Mater.* **2006**, *18*, 2740−2749.

(7) (a) Jung, J.; Jeon, J.; Sridhar, V.; Oh, I. *Carbon* **2011**, *49*, 279−1289. (b) Zarrin, H.; Higgins, D.; Jun, Y.; Chen, Z.; Fowler, M. *J. Phys. Chem. C* **2011**, *115*, 20774−20781.

(8) Ravikumar; Scott, K. *Chem. Commun.* **2012**, *48*, 5584−5586.

(9) Zhu, Y.; Murali, S.; Cai, W.; Li, X.; Suk, J. W.; Potts, J. R.; Ruoff, R. S. *Adv. Mater.* **2010**, *22*, 3906−3924.

(10) (a) Karim, M. R.; Shinoda, H.; Nakai, M.; Hatakeyama, K.; Kamihata, H.; Matsui, T.; Taniguchi, T.; Koinuma, M.; Kuroiwa, K.; Kurmoo, M.; Matsumoto, Y.; Hayami, S. *Adv. Funct. Mater.* **2013**, *23*, 323−332. (b) Matsumoto, Y.; Koinuma, M.; Kim, S. Y.; Watanabe, Y.; Taniguchi, T.; Hatakeyama, K.; Tateishi, H.; Ida, S. *ACS Appl. Mater. Interfaces* **2010**, *2*, 3461−3466.

(11) (a) Jung, I.; Dikin, D. A.; Piner, R. D.; Ruoff, R. S. *Nano Lett.* **2008**, *8*, 4283−4287. (b) Gomez-Navarro, C.; Weitz, R. T.; Bittner, A. M.; Scolari, M.; Mews, A.; Burghard, M.; Kern, K. *Nano Lett.* **2007**, *7*, 3499−3503.

(12) Hummers, W. S.; Offeman, R. E. *J. Am. Chem. Soc.* **1958**, *80*, 1339.

(13) Gao, W.; Singh, N.; Song, L.; Liu, Z.; Reddy, A. L. M.; Ci, L.; Vajtai, R.; Zhang, Q.; Wei, B.; Ajayan, P. M. *Nat. Nanotechnol.* **2011**, *6*, 496−500.

(14) (a) Aoki, Y.; Habazaki, H.; Nagata, S.; Nakao, A.; Kunitake, T.; Yamaguchi, S. *J. Am. Chem. Soc.* **2011**, *133*, 3471−3479. (b) Kitamura, N.; Amezawa, K.; Tomii, Y.; Yamamoto, N. *Solid State Ionics* **2003**, *162*−*163*, 161−165. (c) Nowick, A. S.; Vaysley, A. V. *Solid State Ionics* **1997**, *97*, 17−26. (d) Bonanos, N. *Solid State Ionics* **1992**, *53*−*56*, 967−974. (e) Shin, S.; Huang, H. H.; Ishigame, M. *Solid State Ionics* **1990**, *40*−*41*, 910−913.

(15) Yamada, T.; Sadakiyo, M.; Kitagawa, H. *J. Am. Chem. Soc.* **2009**, *131*, 3144−3145.

(16) (a) Maier, J. *Solid State Ionics* **1987**, *23*, 59−67. (b) Maier, J. *Solid State Ionics* **2003**, *157*, 327−334.

(17) Mermoux, M.; Chabre, Y.; Rousseau, A. *Carbon* **1991**, *29*, 469−474.

(18) (a) Lerf, A.; Buchsteiner, A.; Pieper, J.; Schottl, S.; Dekany, I.; Szabo, T.; Boehm, H. P. *J. Phys. Chem. Solids* **2006**, *67*, 1106−1110. (b) Buchsteiner, A.; Lerf, A.; Pieper, J. *J. Phys. Chem. B* **2006**, *110*, 22328−22338.

(19) (a) Kelly, A. *Strong Solids*; Oxford University Press: Oxford, U.K., 1966. (b) Vilatela, J. J.; Elliott, J. A.; Windle, A. H. *ACS Nano* **2011**, *5*, 1921−1927.

(20) Matsui, J.; Miyata, H.; Hanaoka, Y.; Miyashita, T. *ACS Appl. Mater. Interfaces* **2011**, *3*, 1394−1397.

(21) Cote, L. J.; Kim, F.; Huang, J. *J. Am. Chem. Soc.* **2009**, *131*, 1043−1049.

(22) Koinuma, M.; Ogata, C.; Kamei, Y.; Hatakeyama, K.; Tateishi, H.; Watanabe, Y.; Taniguchi, T.; Gezuhara, K.; Hayami, S.; Funatsu, A.; Sakata, M.; Kuwahara, Y.; Kurihara, S.; Matsumoto, Y. *J. Phys. Chem. C* **2012**, *116*, 19822−19827.